Anal. Bioanal. Electrochem., Vol. 15, No. 10, 2023, 891-913
https://www.doi.org/10.22034/abec.2023.708677

Analytical & Bioanalytical Electrochemistry

Full Paper

Evaluation of the Inhibiting Power of Essential Oil Extracted from Cloves (Syzygium Aromaticum) on Corrosion of Steel C24 In Medium HCl 1M

Malick Bathily,[1,2] Khaly Cissé,[1] Youssef Youssefi,[2] Omar Ou-ani,[2] Lahcen Oucheikh,[2] Baba Ngom,[3] Mohamed Znini,[2] Diadioly Gassama,[1] and Jean Costa[4]

[1]*Department of Physics and Chemistry, UFR Sciences and Technologies, Iba Der THIAM University of Thies, Thies, Senegal*
[2]*Laboratory of Natural Substances & Synthesis and Molecular Modeling, Faculty of Sciences and Techniques, Moulay Ismail University of Meknes, BP 509 Boutalamine, Errachidia 52003, Morocco*
[3]*Laboratory of Water and Environmental Sciences and Technologies (LaSTEE), polytechnic school of Thiès, Thiès, Senegal*
[4]*Laboratory of Chemistry of Natural Products, UMR CNRS 6134, Faculty of Sciences and Techniques, University of Corte, Corte, France*

*Corresponding Author, Tel.: +221775363311
E-Mail: malickbathily@gmail.com

Received: 6 May 2023 / Received in revised form: 29 September 2023 / Accepted: 10 October 2023 / Published online: 31 October 2023

Abstract- The objective of this research is to enhance the value of the clove tree (Syzygium aromaticum), an aromatic and medicinal plant found in Senegal. The focus is on assessing the inhibitory effect of the essential oil extracted from clove on C24 carbon steel in a 1M HCl medium. In the initial phase of the study, essential oil was extracted from the cloves through hydrodistillation utilizing a Clevenger-type extractor. These extractions yielded an average extraction rate of 11.7%, a notably commendable figure when compared to various data reported in existing literature. Subsequently, the extracted essential oil underwent characterization employing standard chromatographic techniques (GC/IR, GC/MS). This allowed for identification of the chemical compounds constituting the essential oil, with major compounds identified as Eugenol (64.97%), Caryophyllene (24.15%), and Acetyleneugenol (6.19%). The research delved into investigating the inhibitory impact of clove essential oil on C24 steel in a 1M HCl medium using electrochemical techniques. The outcomes of this investigation indicated an optimal efficacy of 88.52% for an essential oil concentration of 4g/L at 290K. Furthermore, the study assessed the influence of temperature on the inhibitory

properties of the essential oil across a temperature spectrum of 290 to 338 K. Within this temperature range, a marginal reduction in efficiency was noted with increasing temperature, ultimately 79.92% at 328 K. Subsequently, thermodynamic parameters were computed. The graphical representation of the distinct isotherms demonstrated that the adsorption of the essential oil adhered to the Langmuir isotherm. The results underscored a blended adsorption characteristic of this essential oil.

Keywords- Clove; Inhibitor; Essential oil; Corrosion; Electrochemical methods; Steel

1. INTRODUCTION

Corrosion is defined as the process of deterioration in metallic materials due to either physical attacks or chemical reactions with their surrounding environment [1]. This corrosive phenomenon predominantly impacts various industrial sectors such as construction, automotive, public works, shipbuilding, and petrochemical industries [2]. Steel, a widely utilized material in these sectors, is highly susceptible to corrosion, resulting in significant financial losses annually, often amounting to thousands of dollars.

Notably, the industrial sector extensively employs aggressive solutions, as hydrochloric acid, for pickling operations, clean with acid, removal of localized deposits, and stimulation of oil wells [3]. This aggressive nature of acid solutions, particularly in the presence of steels, necessitated the exploration of methods to safeguard steels against corrosion in acidic environments. One of the protective approaches involves the use of corrosion inhibitors. These inhibitors, when added in minimal concentrations within corrosive settings, mitigate or hinder the metal's reaction with its surroundings. It's worth mentioning that the majority of inhibitors employed in acidic environments are of the synthetic organic variety [4-10]. Typically, these synthetic inhibitors demonstrate effective anticorrosive properties. However, a significant drawback lies in their high toxicity to both humans and the environment. To address these concerns, recent research has shifted towards exploring natural substances as corrosion inhibitors. These natural substances are generally non-toxic and exhibit good biodegradability. Within our research institution, substantial efforts have been dedicated to investigating the potential of these natural substances as corrosion inhibitors for metallic materials [11-14].

Specifically focusing on vegetable oils and essential oils, numerous studies have been conducted in recent years to assess their corrosion inhibitory effects [15-21]. Furthermore, in a previous study conducted by our team, we evaluated the inhibitory action of essential oil extracted from *Eucalyptus globulus* leaves on carbon steel in a 1M HCl medium using a gravimetric method [22]. This study revealed an optimal efficiency of 89.03% at a concentration of 1.6 g/L and a temperature of 298 K.

In this current study, our objective is twofold. Firstly, we aim to explore the potential of utilizing locally available plants by extracting essential oil from clove buds. Secondly, we intend to investigate the inhibitory action of clove essential oil on the corrosion of C24 carbon steel in a 1M hydrochloric acid (HCl) medium.

2. MATERIALS AND METHODS

2.1. Method of extraction of the essential oil

The plant material used for the extraction of the inhibitor is obtained from the flower buds of the wallflower (*Syzygium aromaticum*), commonly known as cloves. Cloves collected in Dakar, Senegal, were cleaned, sorted and cleared of all artifacts. The plant material was then ground into powder form for extraction.

The essential oil extraction was performed through hydrodistillation, utilizing a Clevenger-type apparatus following the methodology outlined in the European Pharmacopoeia [23]. The extraction procedure involved 300 grams of plant material submerged in 2.4 liters of water, brought to a boil using a heating flask. The temperature was limited to the boiling point of water (100°C). The extraction duration was set at three hours.

The resulting essential oil (EO) was carefully dried using anhydrous sodium sulfate (Na_2SO_4) and then stored in temperature-controlled conditions (4°C) within securely sealed bottles, shielded from light, until its intended usage.

To assess the efficiency of the extraction process, the yield of essential oil was calculated relative to the mass of dry plant matter. The yield is expressed as the quantity of essential oil (in grams) obtained for every 300 grams of dry plant matter (DV).

$$R\,(\%) = \frac{m(HE)}{m(MV)} \times 100 \qquad \text{Eq. 1}$$

2.2. Characterization of the essential oil

The analysis of clove essential oil involved gas chromatography (GC) using the Perkin Elmer Autosystem GC (Walhton, MA, USA) XL chromatograph. The GC system was equipped with a single injector, flame ionization detectors (FID) for compound detection, and fused silica capillary columns (60 m × 0.22 mm, film thickness 0.25 μm) with different stationary phases, including polar (Rtx-Wax, polyethylene glycol) and apolar (Rtw-1, polydimethyl siloxane). The injector and detector were set to a temperature of 280°C, and the oven temperature was programmed to increase from 60°C to 230°C at a rate of 2°C/min, maintaining 230°C for 35 minutes. Helium was employed as the carrier gas at a flow rate of 1 ml/min. Injection was carried out using a split mode with a split ratio of 1/50, and the injected oil volume was 0.1 μL. For each compound, both polar and apolar retention indices (Ir_p and Ir_a) were determined during the analysis.

Clove essential oil samples were subjected to analysis using gas chromatography/mass spectrometry (GC/MS) through a Perkin Elmer Autosystem XL chromatograph coupled to an injector. Detection was achieved using a quadrupole analyzer directly linked to an automated Perkin Elmer TurboMass detector, equipped with two columns (60 m × 0.22 mm d.i; film thickness: 0.25 μm) with polar (Rtx-Wax, polyethylene glycol) and apolar (Rtw-1, polydimethyl siloxane) stationary phases. Helium was utilized as the vector gas (1 ml/min).

The ion source temperature was set at 150°C, and the oven temperature was programmed to increase from 60°C to 230°C at a rate of 2°C/min, maintaining 230°C for 35 minutes. The injector operated in split mode (1/80) at 280°C, with an injection volume of 0.2 µL of pure oil. The ionization energy was set at 70 eV. Mass spectra acquired by electronic impact were within the 35-350 Da mass range.

The identification of sample compounds was conducted using two methods:

(i) Based on the comparison of their retention indices (Ir_a and Ir_p) on the apolar and polar columns respectively, determined in relation to a standard range of alkanes; in comparison with the retention indices of reference compounds or those found in the literature [24].

(ii) By comparing their resulting mass spectra with those of reference products contained in a commercial library [25], and by cross-referencing the mass spectra with those in our proprietary library.

Relative percentages of components were calculated based on the peak areas of clove compounds on the two capillary columns, Rtx-1 and Rtx-Wax, without applying any correction factors. These percentages were then compared with those of reference products (measured in the laboratory or described in the literature (Ir_l)).

2.3. Corrosion test

The corrosive medium used for corrosion tests is a one molar solution of hydrochloric acid (HCl). This solution is prepared by diluting a commercial concentrated hydrochloric acid solution with a density of 1.19, molar mass of 36.46 g/mol, and mass percentage of 37%, using distilled water.

The corrosion experiments were conducted on mild carbon steel plates of C24 grade, primarily composed of iron. The chemical composition of the steel (mass percentage) includes C = 0.2, P = 0.005, N = 0.07, and S = 0.05.

Prior to each corrosion test, the steel sample representing the working electrode underwent mechanical grinding with sequential grades of emery paper (400, 600, 1200, 1500, and 2000 grit). Subsequently, it was thoroughly rinsed, degreased with distilled water and acetone, and then dried.

Electrochemical measurements were carried out at a controlled temperature of 290 ± 2 K in a conventional cylindrical Pyrex glass cell containing three electrolytic electrodes: a disc-shaped work electrode cut from C24 steel with a surface area of 1 cm^2 and coated in epoxy resin, a saturated calomel electrode (SCE) utilized as a reference electrode, and a platinum electrode functioning as the counter electrode. All electrochemical measurements were performed using a potentiostat (model SP-150) controlled by EC-Lab software. Potential measurements were taken relative to the potential value of the reference electrode.

It's crucial to emphasize that before initiating each electrochemical corrosion test, the steel sample was immersed in the solution for a duration of 30 minutes at open circuit potential (OCP) to achieve a stable and steady state of the system before proceeding with the electrochemical measurements.

2.4. Stationary method: polarization curves

Polarization curve investigations using Tafel's methodology were conducted on C24 steel in a 1M HCl electrolyte under two conditions: without the presence of any substance and with varying concentrations of clove essential oil (ranging from 0.25 to 4 g/L) as a corrosion inhibitor. The polarization curves included cathodic and anodic segments, delineated by modifying the electrode potential within the range of -800 mV to 0 V concerning the reference electrode at the open circuit potential. These measurements were made at a scan rate of 1 mV/s. Utilizing Tafel plots, the corrosion current was deduced by extending the anodic and cathodic Tafel lines to a specific point, enabling the calculation of current density (log I_{corr}) and the respective corrosion potential (E_{corr}) for each concentration of the inhibitor, as well as for 1M HCl in isolation.

2.5. Transient methods (electrochemical impedance spectroscopy (EIS))

Electrochemical impedance spectroscopy (EIS) measurements were conducted in a 1M HCl solution, both in the absence and presence of varying inhibitor concentrations (ranging from 0.25 to 4 g/L). The working electrode, a steel sample with a surface area of 1 cm^2 exposed to the solution, was utilized in the tests. The EIS assessments covered a frequency range from 100 KHz to 10 mHz at the open circuit potential, employing a signal amplitude of 10 mV. The Nyquist plots provided the values for charge transfer resistance (R_{tc}) and double layer capacitance (C_{dc}). R_{tc} values were calculated based on the impedance disparity between lower and higher frequencies [26]. Each electrochemical technique was repeated a minimum of three times for both the blank and each concentration to ensure result reproducibility.

3. RESULTS AND DISCUSSION

3.1.Yield of the extractions carried out

The extraction of cloves gave an essential oil of light-yellow color, with an odor quite striking and very strong. The average yield of these extractions is 11.7%, a yield that is quite consistent with values found in the literature. Muchamad et al [27] found for their studies on cloves yields of 13.4% for their samples from Comoros and Zanzibar, 14.3% for samples from Madagascar and 4.1% for their samples from Indonesia. Yields differed depending on the origin of the sample.

3.2. Chemical composition of the essential oil of cloves

The identification of the components of the EO extracted from cloves was carried out by the usual chromatographic techniques (GC/IR and GC/MS). Through these techniques, 19 constituents were identified, constituting 99.78% of the EO's complete composition. The identification process relied on comparing mass spectra and polar as well as apolar retention indices (Irp and Ira) of the constituents with those of established reference compounds (Table 1).

Table 1. Chemical composition of the essential oil of clove

No.	**Compounds**	**$Ira_{(l)}$**	**$Ira_{(exp)}$**	**%**
1	2-nonanone	1071	1079	0.02
2	Methyl salicylate	1167	1130	0.01
3	Eugenol	1331	1338	64.97
4	α-copaene	1379	1378	0.40
5	Caryophyllene	1421	1424	24.15
6	Cis-β-farnesene	1447	1429	0.05
7	Cis-muurola-4(15),5-diene	1454	1449	0.02
8	α-muurolene	1451	1454	2.37
9	γ-muurolene*	1471	1472	0.13
10	Cadina-1(6),4-diene*	1468	1472	0.01
11	β-selinene	1482	1479	0.03
12	Acetyleneugenol	1485	1487	6.19
13	Germacrene D	1481	1487	0.32
14	α-farnesene	1496	1493	0.55
15	γ-cadinene	1507	1506	0.03
16	Calamene	1510	1509	0.04
17	δ-cadiene	1520	1516	0.27
18	Cubebene	1525	1527	0.04
19	Caryophyllene oxide	1578	1575	0.18
Total identified compounds				99.78
Hydrocarbon compounds				
Sesquiterpenes				28.41
Total hydrocarbon compounds				28.41
Oxygenated compounds				
Ketones				0.02
Esters				71.17
Oxide				0.18
Total oxygenated compounds				71.37

Ira(exp): Experimental retention indices on apolar column (Rtx-1)
Ira(l): Apolar retention indices from the literature
Relative abundances were calculated on the basis of experimental Ira except for compounds marked * giving rise to co-elution where polar column retention indices Irp (Rtx-Wax) were used: γ-muurolene Irp: 1681, Cadina-1(6),4-diene IRp: 1712.

Upon analyzing Table 1, it becomes evident that the clove essential oil (EO) is distinguished by a substantial presence of oxygenated compounds, comprising five compounds and representing 71.37% of the composition. Additionally, a considerable fraction of sesquiterpene compounds, consisting of 14 sesquiterpenes, constitutes approximately 28.41% of the total chemical composition of the oil. Notably, the EO lacks any monoterpene fraction. This EO is also characterized by the presence of an Esther named Eugenol at a very high content. The major constituents that characterize this EO are: Eugenol (64.97%), Caryophyllene (24.15%), Acetyleneugenol (6.19%).

3.3. Open circuit potential

In Figure 1, the open circuit potential (OCP) dynamics of C24 steel over time are illustrated, comparing scenarios with and without varying concentrations of clove essential oil (EO) serving as a corrosion inhibitor. It is observed that in the presence of EO, C24 steel displays a more positively shifted OCP compared to the blank solution. This shift signifies that the essential oil diminishes the tendency of C24 steel to dissolve in the corrosive solution.

The graphical representations of the OCP evolution show that C24 steel can reach a quasi-stable OCP within 30 min of immersion. As a result, all electrochemical measurements conducted in this study were preceded by a 30-minute OCP measurement to establish a stable baseline.

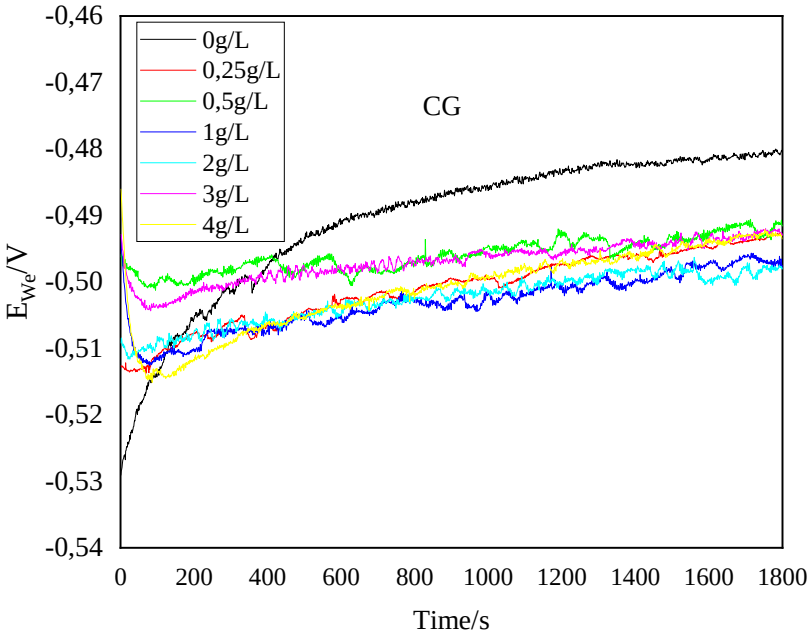

Figure 1. Monitoring of the corrosion potential of C24 steels in 1M HCl solutions in the absence and presence of different concentrations of Clove EO at 290 K

3.4. Study by electrochemical impedance spectroscopy (EIS)

3.4.1. Effect of concentration

The effect of clove EO concentration was investigated by EIS electrochemical impedance spectroscopy over a concentration range of 0.25 to 4g/L. Figure 2 shows the electrochemical impedance plots in the Nyquist plane and Figure 3, they are displayed in the Bode plane. These plots represent the behavior of C24 steel immersed in a 1M HCl solution at different inhibitor concentrations. The measurements were taken after a 30-minute immersion at a temperature of 290 K, with the potential held at open circuit over a frequency span ranging from 100 KHz to 10 mHz.

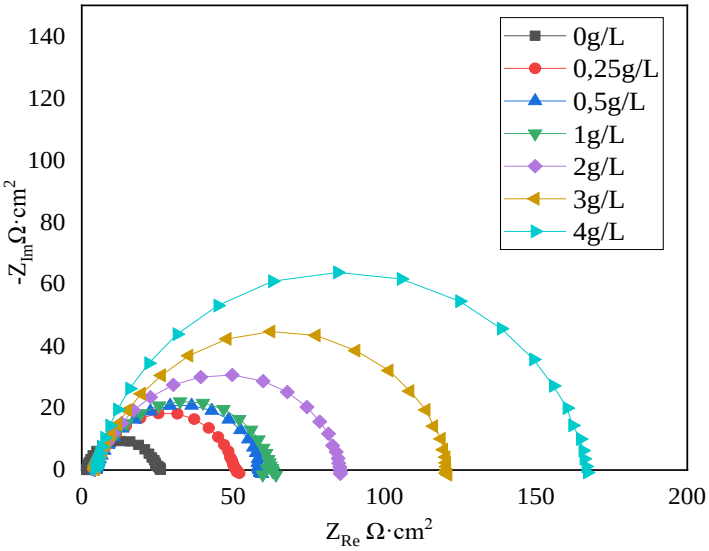

Figure 2. Representation of impedance diagrams in the Nyquist plane of C24 steel in 1M HCl in the absence and presence of different concentration of CG HE at 290 K

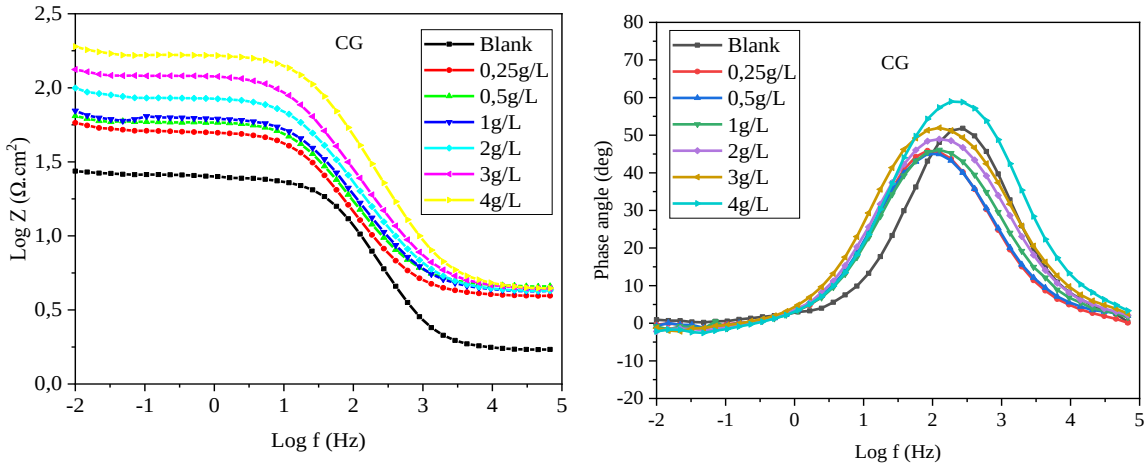

Figure 3. Bode (a) and phase angle (b) curves for the corrosion of C24 steel in 1 M HCl at different Clove essential oil concentration at 290 K

In Figure 2, it's evident that the introduction of clove essential oil (EO) as a corrosion inhibitor leads to an enlargement of the semicircle compared to the blank solution. The diameter of the Nyquist plots increases proportionally with the inhibitor concentration. This phenomenon signifies an escalation in the resistance against metal dissolution in the corrosive solution, indicating substantial adsorption of the inhibitor on the metal surface. The presence of a single capacitive loop suggests that the adsorption process studied is controlled by a charge transfer mechanism at the electrode/solution interface [28]. Additionally, the absolute and phase angle Bode diagrams (Figure 3) were generated. The absolute Bode diagram (Figure 3a) demonstrates an augmentation in absolute impedance values with increasing inhibitor concentration across both low and high frequencies. In Figure 3b, an increase in the phase angle is observed with rising inhibitor concentration, along with a shift of the phase angle peak towards lower frequencies. These findings validate that a higher inhibitor concentration offers enhanced protection to the metal interface.

To comprehensively comprehend the impedance characteristics variations observed in each response derived from the EIS spectra, an electrical circuit model representing the metal/solution interface was analyzed across all frequencies using Ec-Lab software, as presented in Figure 4. This electrical circuit model, frequently employed in research concerning natural inhibitors in acidic conditions [29-31], incorporates parameters such as electrolyte resistance (R_s), charge transfer resistance (R_{tc}), and double layer capacitance (C_{dc}).

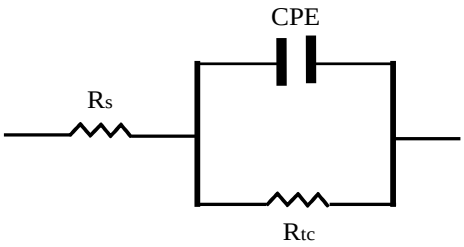

Figure 4. Equivalent electrical circuit for modeling impedance spectra. Rs = Electrolyte resistance; R_{tc} = Charge transfer resistance; CPE = Constant phase element

In Table 2, we present crucial impedance parameters including charge transfer resistance (R_{tc}), electrolyte resistance (R_s), double layer capacitance (C_{dc}), and the corresponding inhibition efficiency (IE) in relation to the inhibitor concentration. The inhibition efficiency (IE) is calculated based on the charge transfer resistance using the following relation [32]:

$$IE = \frac{R't - Rt}{R't} \times 100 = 100 \times \theta \qquad \text{Eq. 2}$$

R_t and R'_t are the values of the charge transfer resistance without and with the inhibitor, respectively.

The values for charge transfer resistance (R_{tc}) and double layer capacitance (C_{dc}) were derived from Nyquist plots. The resistance values (R_{tc}) were calculated by evaluating the

impedance difference at lower and higher frequencies [26]. The double layer capacitance (C_{dc}) and the frequency where the imaginary component of the impedance is maximum ($-Z_{max}$) are determined using the equation (Eq. 3):

$$C_{dc} = \frac{1}{\omega . Rt} \qquad \text{Eq. 3}$$

where $\omega = 2.\pi.Z_{max}$ Z_{max} is the frequency for which the imaginary part of the impedance is maximum, C_{dc}: Double layer capacitance ($\mu F.cm^{-2}$) and R_{tc}: Charge transfer resistance ($\Omega.Cm^2$).

The time constant (τ) is calculated by the following relationship [33-34]:

$$\tau = C_{dc}\, R_{tc} \qquad \text{Eq. 4}$$

Table 2. Impedance parameters and inhibition efficiency values for C24 steel in 1M HCl in the absence and presence of different clove EO concentrations at 290 K

C (g/L)	R_s ($\Omega.cm^2$)	R_{tc} ($\Omega.cm^2$)	C_{dc} ($\mu F.cm^{-2}$)	Z_{max} (HZ)	n	τ (s)	θ	Ei%
0	1.807	22.75	111.7	62.63	0.3523	0.0025		
0.25	4.239	44.61	112.6	31.68	0.5842	0.0050	0.49	49.00
0.5	4.933	51.21	101.2	30.71	0.6399	0.0052	0.56	55.58
1	4.609	54.49	86.34	33.83	0.7563	0.0047	0.58	58.25
2	4.651	76.4	70.5	29.55	1.019	0.0054	0.70	70.22
3	4.878	108.4	58.01	25.31	1.17	0.0063	0.79	79.01
4	4.816	153.7	29.61	34.97	0.831	0.0046	0.85	85.20

Upon examining the EIS data outlined in Table 2, a noticeable trend is observed in the charge transfer resistance (R_{ct}) values. As the concentration of the inhibitor increases, the R_{ct} values also increase, peaking at 153.7 $\Omega.cm^2$ for a concentration of 4 g/L of essential oil. This rise in charge transfer resistance indicates a reduction in the active surface area available for the corrosion reaction, consequently leading to a decrease in the corrosion rate [35]. Moreover, this increase in R_{ct} is directly proportional to the effectiveness of the inhibitor in hindering the corrosion process. The addition of 0.25 $g.L^{-1}$ of clove essential oil to the electrolyte reduces the corrosion rate by 49% and the maximum efficiency achieved is 85.20% at 4 $g.L^{-1}$.

3.4.2. Effect of temperature

The influence of temperature is a critical factor in understanding the effectiveness of inhibitors, and this aspect has been extensively studied in previous research [36-38]. In our study, we aimed to investigate the impact of temperature on the inhibitory properties of clove essential oil concerning C24 steel in a 1M HCl medium.

Indeed, it's well-established that an increase in temperature tends to accelerate the corrosion rate. This temperature-dependent effect can lead to alterations in the performance of corrosion inhibitors [38]. In our investigation, we conducted electrochemical impedance spectroscopy (EIS) studies under varying temperatures, ranging from 290 to 328 K. Both absence and presence of 4 g/L of essential oil were considered. These electrochemical measurements were carried out after allowing the samples to immerse in the solution for 30 minutes at the specified temperature, maintaining the open circuit potential (OCP) to establish an equilibrium state. Temperature control was achieved using a LAUDA water bath model Eco Silver.

In Figure 5, we have depicted the electrochemical impedance diagrams in the Nyquist plane for C24 steel in 1M HCl without the inhibitor (Figure 5) and in the presence of 4 g/L of the inhibitor (Figure 5), across the temperature range from 290 to 328 K.

The corrosion parameters charge transfer resistance (R_{tc}), electrolyte resistance Rs, double layer capacitance C_{dc} and inhibitory efficiency (IE) are given in Table 3.

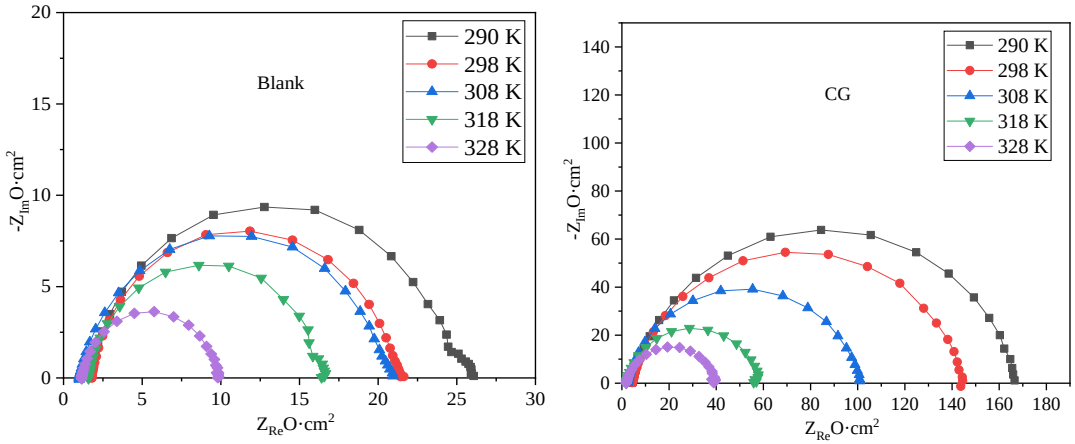

Figure 5. Impedance diagrams in the Nyquist plane of C24 steel in 1M HCl in the absence and presence of 4g/L clove EO at different temperatures

Table 3. Impedance parameters and inhibition efficiency values for C24 steel in 1M HCL in the absence and presence of 4g/L clove EO at different temperatures

Solution	Blank					4g/L				
T(K)	290	298	308	318	328	290	298	308	318	328
Rs ($\Omega.cm^2$)	1.807	1.879	1.068	1.666	1.214	4.816	4.831	2.61	2.014	1.958
Rtc($\Omega.cm^2$)	22.75	18.95	18.72	14.29	8.247	153.7	133.2	94.13	54	35.54
Cdc ($\mu F.cm^{-2}$)	111.7	121	216	122	121	29.61	37.85	39.45	42.89	66.33
Ei% (100 θ)						85.20	85.77	80.11	73.54	76.80

Upon analyzing the electrochemical impedance diagrams plotted in the Nyquist plane, it is evident for both the blank solution and the solution with 4g/L inhibitor that the diameter of the Nyquist semicircles decreases with rising temperature. This decrease in diameter signifies a reduction in the resistance to the dissolution of the metal in the corrosive solution, consequently resulting in higher corrosion rates as temperature increases. Notably, the fundamental shape of the Nyquist diagram remains consistent in the absence and presence of inhibitors.

To analyze the experimental data and extract the electrochemical parameters of interest, the same equivalent circuit as illustrated in Figure 4 was employed. The obtained values are detailed in Table 3. The results from the EIS measurements in Table 3 affirm these observations, showcasing a decrease in charge transfer resistance (R_{tc}) with increasing temperature. Specifically, R_{tc} decreases to 8.247 Ω.cm² for the blank and 35.54 Ω.cm² for the solution with 4g/L at a temperature of 328 K.

In terms of inhibitory efficiency, a minor increase in efficiency is observed at 298 K, followed by a gradual decline until reaching a minimum of 73.54% at 318 K and 76.80% at 328 K. These results indicate that clove essential oil serves as a commendable inhibitor within the chosen temperature range. The observed inhomogeneous variation and marginal loss of efficiency with increasing temperature could be attributed to the combined effect of two adsorption modes during inhibitor adsorption: chemisorption and physisorption, with physisorption being dominant. This phenomenon aligns with the findings of Ivanov et al [39] and Putilova et al [40], suggesting a shift in the nature of adsorption with temperature. The inhibitor is likely physically adsorbed at lower temperatures, while chemisorption becomes more prominent at elevated temperatures.

3.5. Polarization curves

3.5.1. Effect of concentration

In this study, we also examined the potentiodynamic polarization curves of C24 steel in a 1M HCl solution both in the presence and absence of varying concentrations of clove essential oil. These measurements were conducted after a 30-minute immersion at the free corrosion potential and with stirring, and the results are illustrated in Figure 6.

For each concentration of clove essential oil in 1M HCl, we determined critical parameters such as corrosion potential (E_{corr}), current density (I_{corr}), cathodic and anodic Tafel slopes (βc and βa), corrosion rate (V_{corr}), and inhibitory efficiency (IE). The calculated inhibitory efficiency (IE) is derived from the following equation [32]:

$$IE = \frac{I_{corr} - I_{corr}^{inh}}{I_{corr}} \times 100 \qquad \text{Eq. 5}$$

I_{corr} and I_{corr}^{inh} represent respectively the corrosion current densities in the absence and presence of inhibitor.

The corrosion rate (or corrosion rate) V_{corr} in mm/year is obtained with the following formula:

$$V_{corr} = \frac{I_{corr} \times M}{d \times V} \times 3270 \qquad \text{Eq. 6}$$

M representing the mass in g, d the density (g/cm^3), V the volume in cm^3 and with: 3270 = 0.01 × [1 year (in second) / 96497.8] and 1F = 96497.6C

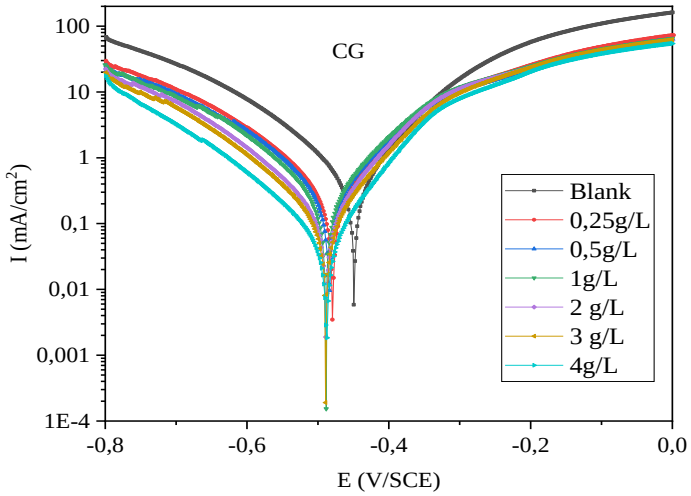

Figure 6. Tafel polarization curves of C24 steel in 1M HCl in the absence and presence of different concentration of CG HE at 290 K

Table 4. Electrochemical parameters and inhibition efficiency values for C24 steel in 1M HCl in the absence and presence of different HE concentrations of cloves at 290 K

C (g/L)	E_{corr} (mV SCE)	ΔE (mV)	I_{corr} (µA cm²)	βc (mV)	βa (mV)	Rp (Ω.cm)^2	V (mm/year)	θ	IE (%)
0	-449.058	0	679.361	144.7	111.9	40.33	15.778		
0.25	-479.249	-30.191	370.271	141.2	120	76.07	8.600	0.455	45.50
0.5	-479.264	-30.206	339.475	135.6	113.5	79.03	7.884	0.500	50.03
1	-484.358	-35.3	319.778	136.6	116.5	85.38	7.427	0.529	52.93
2	-488.74	-39.682	189.601	130.4	104.2	132.64	4.403	0.721	72.09
3	-489.282	-40.224	144.993	128.1	101.4	169.50	3.367	0.787	78.66
4	-487.862	-38.804	77.991	128.2	92.3	298.77	1.811	0.885	88.52

An analysis of the potentiodynamic polarization curves reveals a notable inhibiting effect on both the anodic and cathodic corrosion mechanisms upon the addition of clove oil. This inhibitory effect is more prominent for the cathodic reaction compared to the anodic reaction,

indicating that the inhibitor reduces both the cathodic dissociation reaction of hydrogen and the anodic dissociation reaction of the metal. Additionally, a slight shift of the corrosion potential (Ec_{orr}) towards the cathodic part is observed. Examining the cathodic branches of the polarization curves, we find that they resemble Tafel lines, implying that the H^+ proton discharge reaction is primarily governed by pure activation kinetics [41].

The potential variation (ΔE) recorded in Table 4 does not exceed 40.22 mV. It's worth noting that in the literature, an inhibitor is generally classified as anodic or cathodic only if its addition to an electrolyte causes a variation in E_{corr} exceeding 85 mV [42-43]. Thus, we can deduce that the inhibitor used in this study exhibits a mixed character in terms of its inhibitory behavior.

The corrosion current density (I_{corr}) undergoes a significant reduction upon the addition of the inhibitor. Its value decreases from 679.36 to 77.99 mA.cm² with the addition of 4g/L of clove essential oil. Simultaneously, this decrease in I_{corr} is accompanied by a decrease in the corrosion rate, leading to a substantial increase in inhibitor efficiency, reaching a maximum of 88.52% at 4 g/L.

These findings from the polarization curves align well with the results obtained from the electrochemical impedance spectroscopy studies, reinforcing the robustness and consistency of the inhibitor's performance across different experimental approaches.

3.5.2. Effect of temperature

Similarly, to the electrochemical impedance spectroscopy, we also investigated the influence of temperature on the inhibitory effectiveness of clove essential oil using the potentiodynamic polarization method. This evaluation was carried out over a temperature range between 290 and 328 K, both in the absence of the inhibitor and in the presence of 4 g/L of essential oil, which was determined as the optimum concentration at 290 K. The measurements were conducted after allowing a 30-minute immersion at the free corrosion potential and under agitation.

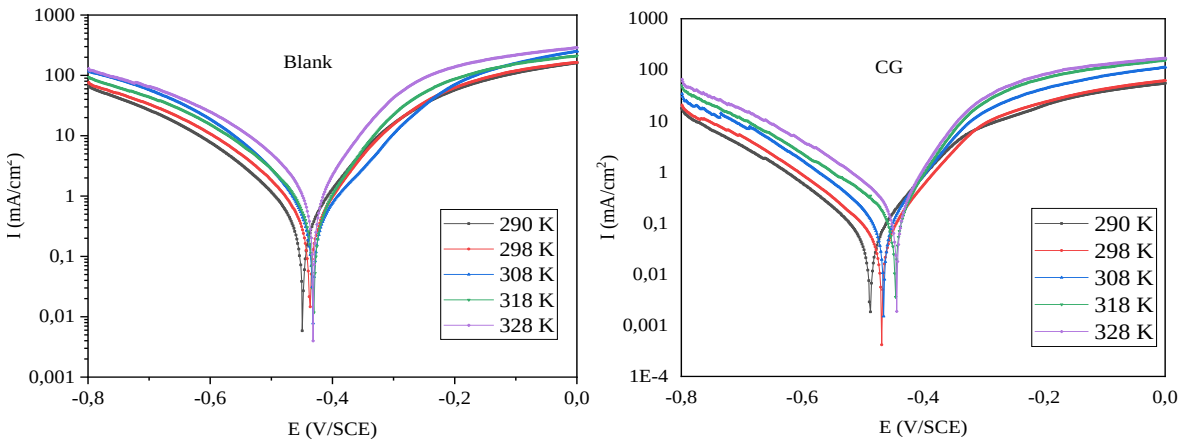

Figure 7. Tafel polarization curves of C24 steel in 1M HCl in the absence (Blank) and presence of 4 g/L clove EO at different temperatures

In Figure 7, we have graphically represented the Tafel polarization curves for C24 steel in 1M HCl without the inhibitor (Figure 7a) and in the presence of the inhibitor (Figure 7b) across temperatures ranging from 290 to 328 K.

Furthermore, corrosion parameters along with inhibitory efficiency for the various temperatures are summarized in Table 5. These parameters provide valuable insights into how the inhibitor's effectiveness varies with temperature using the potentiodynamic polarization technique.

Table 5. Electrochemical parameters and inhibition efficiency values for C24 steel in 1M HCl in the absence and presence of different HE concentrations of cloves at 290 K

Solution	Blank	4 g/L	Blank	4 g/L	Blank	4 g/L	Blank	4 g/L	Blank	4 g/L
T (K)	290 K		298 K		308 K		318 K		328 K	
E_{corr} (mV SCE)	-449.058	-487.862	-436.971	-468.536	-431.69	-465.293	-430.687	-445.975	-431.637	-443.843
I_{corr} (μA cm²)	679.361	77.991	773.492	80.477	808.176	143.911	1043.193	243.456	1812.8	363.993
βc (mV)	144.7	128.2	143.5	128.2	119.4	128	145.5	162	148.6	153
βa (mV)	111.9	92.3	109.6	86.4	114.1	86.1	103.9	82.9	106.4	86
V	15.78	1.81	17.97	1.87	18.77	3.34	24.23	5.66	42.11	8.46
Ei%		88.52		89.60		82.19		76.66		79.92

An analysis of the polarization curves presented in Figure 7 reveals that, both in the absence and presence of the inhibitor, there's a shift of the corrosion potential (E_{corr}) towards the anodic region with increasing temperature. The cathodic branches exhibit a consistent parallel nature, indicating the same mechanism for the reduction of H^+ ions on the metal surface at each temperature [44]. Conversely, for the anodic branch, the plots obtained are not parallel, suggesting a possible modification of the anodic dissolution mechanism of the metal with temperature.

As indicated in Table 5, the corrosion current densities (I_{corr}) and corrosion velocities (V_{corr}) increase with temperature. Typically, higher temperatures can lead to increased desorption of absorbed inhibitors and a faster dissolution of the metal [45]. However, it's noteworthy that I_{corr} remains relatively lower in the presence of the inhibitor across all temperatures. These results affirm that clove essential oil effectively inhibits corrosion within the studied temperature range. Moreover, despite the increase in I_{corr} with temperature, the electrode surface remains largely intact after the corrosion tests.

Additionally, the data indicates a slight initial increase in efficiency (89.60%) at 298 K, followed by a minor reduction in efficiency, reaching 79.92% at 328 K. These findings align with the observations from the electrochemical impedance spectroscopy studies, reinforcing the consistency and effectiveness of the inhibitor across different experimental methods.

3.6. Thermodynamic parameters

The determination of thermodynamic parameters offers valuable insights into the mechanism of inhibitor absorption on the metal surface. In acidic solutions, the correlation between the corrosion rate and temperature, following an Arrhenius-type dependence, enables the assessment of the activation energy (E_a) for the corrosion process at various temperatures, both in the absence and presence of the optimal inhibitor concentration. This assessment is performed using the following relationship [46]:

$$V_{corr} = k \exp\left(-\frac{E_a}{RT}\right) \qquad \text{Eq. 7}$$

Here, V_{corr} is the corrosion rate of the steel in mm/year, E_a is the activation energy in kJ/mol, R is the gas constant (8,32 J-K^{-1} -mol^{-1}), k is a pre-exponential factor, T is the absolute temperature in Kelvin (K).

Arrhenius diagrams, represented by [ln(V) =f (1/T)] allow for the determination of apparent activation energies from the slopes. This graph is depicted in Figure 8a.

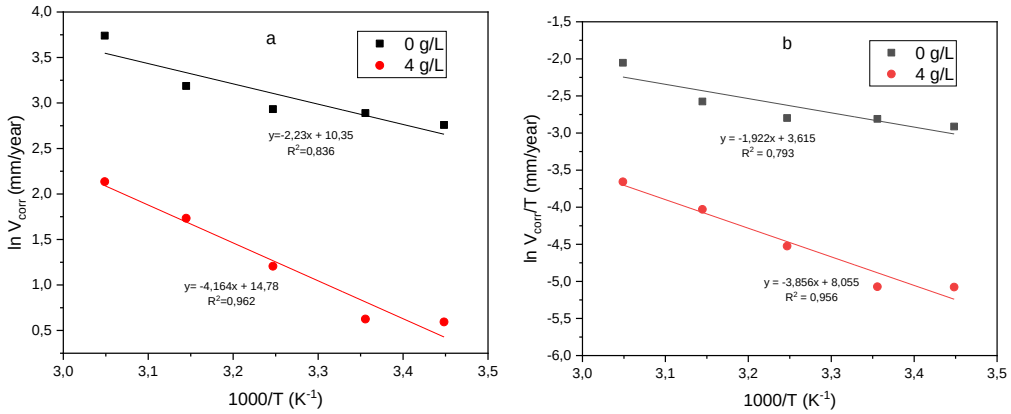

Figure 8. Arrhenius diagrams (a) and transition state diagrams (b) for the corrosion process in 1 M HCl, both in the absence and presence of 4 g/L clove essential oil, at different temperatures. The kinetic parameters of activation for the reaction, namely the enthalpy (ΔH_a°) and the entropy of activation (ΔS_a°), have been determined from the transition state diagrams using the relationship [ln (V/T) = f (1/T)]

To calculate these values, we applied either the Arrhenius transition equation or the equation of the activated complex, as described by the literature [47]:

$$V_{corr} = \frac{RT}{Nh} \exp\left(\frac{\Delta S_a^\circ}{R}\right) \exp\left(-\frac{\Delta H_a^\circ}{RT}\right) \qquad \text{Eq. 8}$$

where h represents the plank constant (6.63 ×10^{-34} J.s), N is Avogadro's number (6.02×10^{23} mol^{-1}), R/N = K_b = 1.38×10 $^{-23}$J·K^{-1} is the Boltzmann constant.

Figure 8b illustrates the relationship of Ln (W/T) as a function of (1/T), where the slope corresponds to -ΔH_a°/R and the intercept at the origin is equal to [Ln (Kb/h) + ΔS_a°/R]. The

calculated values of activation enthalpies $\Delta H_a^\circ$and the activation entropies ΔS_a° are given in Table 6.

Table 6. Thermodynamic parameters of C24 steel in 1M HCl in the absence and presence of 4 g/L clove essential oil

C (g/L)	E_a (KJ. Mol $^{-1}$)	ΔS_a° (KJ. Mol $^{-1}$)	ΔH_a° (KJ. Mol^{-1})
0	18,55	-167,59	15,99
4	34,64	-130,63	32,08

Analyzing the results presented in Table 6, we observe an increase in activation energy in the presence of 4 g/L of the clove essential oil. This rise in activation energy is accompanied by a slight reduction in inhibitory efficiency with increasing temperature. This behavior is indicative of the inhibitor molecules being adsorbed on the steel surface through weak bonding, primarily physisorption [44].

In terms of the thermodynamic parameters (ΔH_a° and ΔS_a°) associated with the dissolution reaction of steel in an acidic medium in the presence of the inhibitor, they are higher than those in the absence of the inhibitor (HCl solution alone). Additionally, both ΔH_a° and E_a exhibit a similar trend, with a minor increase observed compared to the values in the absence of the inhibitor. The enthalpy in the presence of the inhibitor is close to the boundary between physisorption and chemisorption. Therefore, it is plausible to infer that adsorption involves both physical and chemical processes [37], despite physisorption being dominant, which explains the minor loss of efficiency at elevated temperatures, for this reason, the presence of some chemisorption is evident. The positive values of ΔH_a° suggest that the dissolution reaction of steel in 1M HCl is endothermic. Conversely, the relatively high negative values of ΔS_a° imply that imply that the activated complex in the kinetically determining step involves an association rather than a dissociation step. This transition represents a decrease in disorder as we progress from reactants to the activated complex [48-53]. Furthermore, both the activation energy E_a and activation enthalpy ΔH_a° exhibit a parallel variation with the inhibitor concentration. This alignment confirms the thermodynamic relationship linking E_a and ΔH_a° [53]:

$$E_a - \Delta H_a^\circ = RT \qquad \text{Eq. 9}$$

R is the constant of perfect gases (8.32 J.K^{-1} .mol^{-1}), T is the absolute temperature in K.

3.7. Adsorption isotherm and standard free energy of adsorption

To gain a deeper understanding of the adsorption mechanism of clove essential oil and the behavior of these inhibitor molecules on the surface of C24 steel, we conducted tests to fit the data obtained in this study with several adsorption isotherms, including:

- The Langmuir isotherm [C/θ = f(C)], assuming no interaction between the adsorbed molecules on the metal surface.
- The Frumkin adsorption isotherm [θ= f(C)], allowing for some interactions between the adsorbates.
- Temkin's adsorption isotherm [θ = f (Ln C)], representing the effect of multilayer coverage.

The coverage rate (θ) of the metal surface, determined using the Ew/100 ratio [54], was analyzed in relation to the concentration of clove essential oil (C_{inh}). This analysis involved the evaluation of the three aforementioned adsorption isotherms to elucidate the behavior of our essential oil (EO). To ascertain the appropriate adsorption isotherm, presented in graphical form as a linear plot, we considered the correlation coefficient value (R^2) and the slope value, aiming for proximity to 1. Through these analyses, the Langmuir adsorption isotherm, expressed as C/θ = f (C), emerged as the most accurate description of the adsorption behavior of clove essential oil acting as an inhibitor on C24 steel.

In Figure 9, the progression of concentration (C_{inh}) / recovery ratio (θ) is illustrated in relation to the inhibitor concentration (C_{inh}). The resultant curve demonstrated a notable alignment with the Langmuir adsorption isotherm, signifying its appropriateness as the optimal representation of the adsorption behavior of the studied EO. This isotherm is visually depicted as a straight line, exhibiting a slope of approximately 1.108, closely resembling 1, and displaying a high correlation coefficient (R^2) of 0.99.

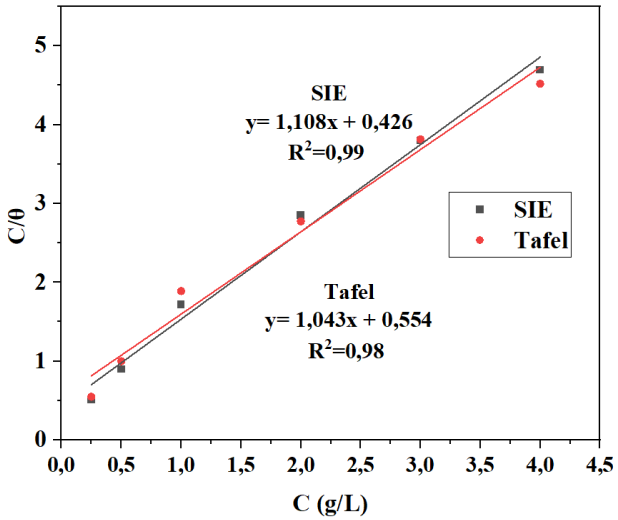

Figure 9. Langmuir adsorption isotherm of C24 carbon steel in 1M HCl in the presence of clove essential oil at 290 K

The Langmuir isotherm equation is expressed by the following formula [55].

$$\frac{C_{inh}}{\theta} = \frac{1}{b} + C_{inh} \qquad \text{Eq. 10}$$

In Eq. 10, the point of intersection with the Cinh / θ axis provides the equilibrium constant's value (b). This constant is linked to the standard free energy of adsorption ΔG°_{ads} through the subsequent equations:

$$\Delta G^{\circ}_{ads} = -RT \log (55.5\ b) \qquad \text{Eq. 11}$$

Here, 55.5 represents the water concentration in mol/L (1000 g/L), and R is the ideal gas constant. Subsequently, we computed the ΔG^{0}_{ads} value, representing the standard free energy of adsorption and characterizing the interactions between inhibitor molecules and the metal surface. These findings are summarized in Table 7.

Table 7. Value of equilibrium constant (b) and standard free energy of adsorption (ΔG^{0}_{ads}) at 290 K in the presence of the studied EO

b (L/g)		ΔG^{0}_{ads} (KJ/Mol)	
EIS	Tafel	EIS	Tafel
2,347	1,805	-18,72	-18,09

When the ΔG_{0} ads values are approximately -20 KJ·mol^{-1} or less negative, the adsorption type is typically physisorption. In this case, the inhibitory action arises from electrostatic interactions between charged molecules and the metal surface. On the other hand, values close to -40 KJ.mol^{-1} or more negative indicate chemisorption, implying the sharing or transfer of electrons from the inhibitor molecules to the metal surface, forming covalent or coordination bonds. For ΔG_{0} ads values falling between -20 and -40 KJ.mol^{-1}, adsorption is a mixture or a combination of both physisorption and chemisorption, demonstrating a complete alternating behavior between the two mechanisms [56-58].

In this research, the calculated negative value of ΔG_{0} ads suggests that the adsorption process of inhibitor molecules and the stability of the adsorbed layer on the steel surface occur spontaneously. Additionally, the ΔG_{0} ads value being less negative than -20 KJ·mol^{-1} indicates that the adsorption mechanism of inhibitor molecules on C24 steel in a 1M HCl medium is likely of a physical nature [59,60]. This assertion gains support from the observed trend where the inhibitory effectiveness of the essential oil diminishes as the temperature rises [61].

4. CONCLUSION

This study primarily focused on assessing the corrosion inhibition potential of clove essential oil on C24 steel in a 1M HCl medium using various electrochemical methods, including the Tafel stationary polarization method and the transient electrochemical impedance spectroscopy (EIS) method.

Our findings revealed a significant reduction in the corrosion of C24 steel with the presence of clove essential oil, leading to an optimal efficiency of 88.52% at 290 K for a concentration of 4 g/L of essential oil. These results, obtained through the Tafel method, were consistent with those obtained using the electrochemical impedance spectroscopy method. The EIS method indicated the formation of a protective film, resulting in increased charge transfer resistance and a reduction in double layer capacity.

Clove essential oil proved to be an effective inhibitor in a 1M HCl medium, demonstrating a minor decrease in inhibitory efficiency with rising temperature, reaching 79.92% for a concentration of 4 g/L at 328K. It is worth noting that clove essential oil remains a reliable inhibitor within the temperature range of 290 to 328 K.

The adsorption of essential oil onto the metal surface conforms to the Langmuir isotherm model. Through the calculation of thermodynamic parameters derived from Arrhenius diagrams, transition state diagrams, Langmuir isotherms, and the observed minor decrease in inhibitory efficiency with temperature, we concluded that the adsorption of essential oil on the metal surface is of a mixed nature. Although physisorption is predominantly influential, chemisorption also contributes to the adsorption process.

Declarations of interest

The authors declare no conflict of interest in this reported work.

REFERENCES

[1] International Organization for Standardization (ISO), ISO 8044 Corrosion of Metals and Alloys - Basic Terms and Definitions, Trilingual version (1999).

[2] D. Benmessaoud Left, M. Zertoubi, A. Irhzo, and M. Azzi, J. Mater. Environ. Sci. 4 (6) (2013) 855.

[3] Z. Bensouda, M. Driouch, M. Sfaira, A. Farah, M. Ebn Touhami, B. Hammouti, and K.M. Emran, Int. J. Electrochem. Sci. 13 (2018) 8198.

[4] A. Nahlé, I. I. Abu-Abdoun, and I. Abdel-Rahman, Int. J. Corrosion (2012) 1.

[5] M. Outirite, M. Lagrenée, M. Lebrini, M. Traisnel, C. Jama, H. Vezin, and F. Bentiss, Electrochim. Acta 55 (2010) 1670.

[6] K. Bouhrira, F. Ouahiba, D. Zerouali, B. Hammouti, M. Zertoubi, and N. Benchat, E-J. Chem. 7 (2010) S35.

[7] Y. Abboud, B. Ihssane, B. Hammouti, A. Abourriche, S. Maoufoud, T. Saffaj, M. Berrada, M. Charrouf, A. Bennamara, and H. Hannache, Desalination and Water Treatment 20 (2010) 35.

[8] B. Zerga, A. Attayibat, M. Sfaira, M. Taleb, B. Hammouti, M. Ebn Touhami, S. Radi, and Z. Rais, J. Appl. Electrochem. 40 (2010) 1575.

[9] L. Herrag, B. Hammouti, S. Elkadiri, A. Aouniti, C. Jama, H. Vezin, and F. Bentiss, Corros. Sci. 52 (2010) 3042.
[10] S. Kertit, H. Es-Soufi, B. Hammouti, and M. Benkaddour, J. Chim. Phys. 95 (1998) 2070-2082.
[11] K. Cissé, J. Mater. Environ. Sci. 9 (2020) 2279.
[12] K. Cissé, D. Gassama, A. A. Diagne, and M. Badji, Int. J. Mater. Sci. Eng. 8 (2020) 17.
[13] D. Gassama, S.M. Seck, I. Yade, M. Fall, and M.B. Diop, Journal of the West African Chemical Soc. 38 (2014) 64.
[14] D. Gassama, M. Fall, I. Yade, S.M. Seck, M. Diagne, and M.B. Diop, Ovidius University Annals of Chem. 27 (2016) 28.
[15] K. Cissé, D. Gassama, A. Thiam, E. H. B. Ndiaye, M. T. Gueye, and M. Fall, Am. J. Phys. Chem. 1 (2021) 6.
[16] D. Ben Hmamou, R. Salghi, A. Zarrouk, B. Hammouti, S.S. Al-Deyab, Lh. Bazzi, H. Zarrok, A. Chakir, and L. Bammou, Int. J. Electrochem. Sci. 7 (2012) 2361.
[17] M. Manssouri, Z. Lakbaibi, M. Znini, Y. E. L. Ouadi, A. Jaafar, and L. Majidi, J. Fail. Anal. Prev. 20 (2020) 1939.
[18] M. Manssouri, A. Laghchimi, A. Ansari, M. Znini, Z. Lakbaibi, Y. E. Ouadi, and L. Majidi, Mediterranean J. Chem. 10 (2020) 253.
[19] Y. N. Otaifah, J. Power Sources 295 (2016) 203.
[20] Ben Hmamou, R. Salghi, Lh. Bazzi, B. Hammouti, S.S. Al-Deyab, L. Bammou, L. Bazzi, and A. Bouyanzer, Int. J. Electrochem. Sci. 7 (2012)1303.
[21] M. Bathily, N. Ngom, D. Gassama, and S. Tamba, American Journal of Applied Chemistry 9 (2021) 65.
[22] M. Bathily, N. Ngom, M. Mbengue, and D. Gassama, Ovidius University Annals of Chem. 34 (2023) 1.
[23] European Pharmacopoeia, Strasbourg: Council of Europe, 7th edition, Volume 1 (2010).
[24] D. Joulain and W.A. König, The Atlas of Spectral Data of Sesquiterpene Hydrocarbons, E-B Verlag, Hamburg, Germany (1998).
[25] D. Hochmuth, D. Joulain, and W.A. König, Library of Mass Finder 2.1, Hamburg (2001).
[26] T. Tsuru, S. Haruyama, and B. Gijutsu, J. Japan Soc. Corros. Eng., 27 (1978) 573.
[27] M. Muchamad, and J. Crouzet, in Ann. Tech., VII Congrès Int. Huiles Essentielles (1982) Fedarom. Grasse, 255.
[28] K. Juttner, and W.J. Lorenz, Mater. Sci. Forum 44 (1989) 191.
[29] K. Azzaoui, E. Mejdoubi, S. Jodeh, A. Lamhamdi, E. Rodriguez-Castellon, M. Algarra, A. Zarrouk, A. Errich, R. Salghi, and H. Lgaz, Corros. Sci. 129 (2017) 70.
[30] G. Monteiro, I. Tavares, M. Carvalho, M. Carvalho, A. Pimentel, P. Santos, E. Vilas Boas, J. Oliveira, V. Capelossi, M. Bilal, and M. Franco, Chem. Eng. Commun. (2022) 1.

[31] M. Benarioua, A. Mihi, N. Bouzeghaia, and M. Naoun, Egypt. J. Pet. 28 (2019) 155.
[32] M. Doubi, A. Dermaj, H. Ramli, D. Chebabe, N. Hajjaji, and A. Srhir, Science Lib. 5 (2013) 2111.
[33] I. Danaee, K.M. Niknejad, and A.A. Attar, J. Mater. Sci. Technol. 29 (2013) 89.
[34] S.T. Selvi, V. Raman, and N. Rajendran, J. Appl. Electrochem. 33 (2003) 1175.
[35] P. Mohan, R. Usha, G.P. Kalaignan, and V.S. Muralidharan, J. Chem. 2013 (2013) 1.
[36] S. Tazi, I. Raissouni, F. Chaoukat, D. Bouchta, A. Dahdouh, R. Elkhamlichi, and H. Douhri, J. Mater. Environ. Sci. 7 (2016) 1642.
[37] K. Cissé, D. Gassama, A. Thiam, M. Bathily, and M. Fall, Chem. Africa, 4 (2021) 379.
[38] M. Znini, M. Bouklah, L. Majidi, S. Kharchouf, A. Aouniti, A. Bouyanzer, B. Hammouti, J. Costa, and S.S. Al-Deyab, Int. J. Electrochem. Sci. 6 (2011) 691.
[39] E.S. Ivanov, Metallurgy, Handbook in Accordance with the State Service of Standard Reference Data, Moscow (1986) 175.
[40] I.N. Putilova, S.A. Balezin and O.P. Barannik, in E. Bishop (Ed.), Metallic Corrosion Inhibitors, Pergamon Press, New York (1960) 2.
[41] G.P. Monteiro, I.M. Tavares, M.C. de Carvalho, M.S. Carvalho, A.B. Pimentel, P.H. Santos, E.V. Vilas Boas, J.R. de Oliveira, V.R. Capelossi, M. Bilal, and M. Franco, Chem. Eng. Commun. (2022).
[42] A.K. Satapathy, G. Gunasekaran, S.C. Sahoo, K. Amit, and P.V. Rodrigues, Corros. Sci., 51 (2009) 2848.
[43] N. Perez, Kinetics of activation polarization, Electrochemistry and Corrosion Science, Boston (2004).
[44] S. Ferraa, M. Ouakki, H. Barebita, A. Nimour, M. Cherkaoui, and T. Guedira, Inorg. Chem. Commun. (2021) 132.
[45] M. Ouakki, M. Galai, Z. Benzekri, C. Verma, E. Ech-chihbi, S. Kaya, S. Boukhris, E.E. Ebenso, M.E. Touhami, and M. Cherkaoui, Colloids Surf. A (2020).
[46] P. Sakunthala, S.S. Vivekananthan, M. Gopiraman, N. Sulochana, and A.R. Vincent, J. Surfactants Deterg. 16 (2012) 251.
[47] S.K. Shukla, and M.A. Quraishi, Corros. Sci. 52 (2010) 314.
[48] F. Bentiss, M. Lebrini, H. Vezin, F. Chai, M. Traisnel, and M. Lagrené, Corros. Sci. 51 (2009) 2165.
[49] G.M. Schmid, and H.J. Huang, Corros. Sci. 20 (1980) 1041.
[50] M. Elachouri, M.S. Hajji, M. Salem, S. Kertit, J. Aride, R. Coudert, and E. Essassi, Corros. 52 (1996) 103.
[51] M.H. Hussin, A.A. Rahim, M.N. Mohamad Ibrahim, and N. Brosse, Measurement 78 (2016) 90.
[52] Y. Abboud, O. Tanane, A. El Bouari, R. Salghi, B. Hammouti, A. Chetouani, and S. Jodeh, Corros. Eng. Sci. Technol. 51 (2016) 557.

[53] G.K. Gomma, and M.H. Wahdan, Mater. Chem. Phys. 39 (1995) 209.
[54] M.S. Morad, Corros. Sci. 50 (2008) 436.
[55] I. Langmuir, J. American Chem. Soc. 39 (1947) 1848.
[56] L.N. Putilova, S. A. Balezin, and V. P. Barannik, Metallic Corrosion Inhibitors, Pergamon Press, New York (1960).
[57] I.A. Ammar, and F.M. El-Khorafi, Werkst Korros. 24 (1973) 702.
[58] D.D.N. Singh, R.S. Chadhary, B. Prakash, and C.V. Agarwal, British Corrosion J. 14 (1979) 235.
[59] A. Fouda, G.Y. Elewady, K. Shalabi, and S. Habouba, Int. J. Advanced Res. 2 (2014) 817.
[60] H.L. Wang, H.B. Fan, and J.S. Zheng, Mater. Chem. Phys. 77 (2003) 655.
[61] J. Nakomčić, G. Vastag, A. Shaban, and L. Nyikos, Int. J. Electrochem. Sci. 10 (2015) 5365.